Journal of Building Engineering 95 (2024) 110301

Contents lists available at ScienceDirect

Journal of Building Engineering

journal homepage: www.elsevier.com/locate/jobe

Improving the adhesion of satin XPS to sandstone with customized polyurethane adhesives for sustainable facade cladding and thermal insulation

Álvaro Miguel-Ortega [a,c], Sara Gonzalez-Moreno [b], Jose Manuel Gonzalez-Martin [b], Raquel Arroyo [b], Félix C. García [a], Miriam Trigo-Lopez [a], Saúl Vallejos [a,*]

[a] Departamento de Química, Facultad de Ciencias, Universidad de Burgos, Plaza Misael Bañuelos s/n, 09001, Burgos, Spain
[b] Departamento de Construcciones Arquitectónicas e Ingeniería de la Construcción y del Terreno, Escuela Politécnica Superior, Universidad de Burgos, C/ Villadiego s/n, 09001, Burgos, Spain
[c] Facultad de Ciencias, Universidad Autónoma de Madrid, Calle Francisco Tomás y Valiente 7, 28049, Madrid, Spain

ARTICLE INFO

Keywords:
Siliciclastic sandstone
Single-component PU
Ageing study
Sustainable construction
Polyethylene glycol
Polypropylene glycol
Poly-MDI

ABSTRACT

Six PU adhesives were synthesised with two different polyols (PPG and PEG based) of three molecular weights, namely 400, 1000 and 2000 g mol^{-1}, and MDI, to prepare sandstone-XPS isolating façade panels. The chemical structure, thermal properties, and adhesion properties in the preparation of the panels were evaluated. Both sandstone and XPS are commonly used materials in construction due to their excellent insulating properties, durability, flexibility, water resistance, and aesthetic appeal, making them environmentally attractive. The industry trend is towards using sanded XPS in these panels, as better adhesion is achieved with typical adhesives compared to satin or unsanded XPS. However, this entails waste generation from sanding, a higher panel price and a difference in adhesive consumption from 309 g m^{-2} to 684 g m^{-2} for unsanded (or satin) and sanded XPS, respectively. In this study, all prepared panels exhibit good adhesion properties, even those made with satin XPS. Panels prepared from PPG-based adhesives show better adhesion performance than those made from PEG, reaching 0.52 ± 0.07 N mm^{-2} with the 1000 g mol^{-1} PPG polyol-based adhesive. These highest adhesion properties are due to the optimal balance of flexible and rigid segments in the polymer material structure. The adhesive maintains its high performance even after harsh temperature and humidity conditions. After accelerated ageing with heat, cold and water, the probes retain between 65 and 71 % of the original tensile strength (0.34 ± 0.03, 0.35 ± 0.07 and 0.37 ± 0.01 N $mm^{-2,}$ respectively). This finding suggests an interesting starting point for cost savings associated with sanding and reduction in XPS waste generation, making them economically and environmentally appealing.

Abbreviations

%NCO	Isocyanate index
δ_s	symmetrical bending
ν_{as}	asymmetrical stretching

* Corresponding author.
E-mail address: svallejos@ubu.es (S. Vallejos).

https://doi.org/10.1016/j.jobe.2024.110301
Received 24 May 2024; Received in revised form 23 July 2024; Accepted 26 July 2024
Available online 27 July 2024

ADH_	prepared adhesives
ASTM	American Society for Testing and Materials
ATR	attenuated total reflection
DMSO-d_6	deuterated dimethylsulfoxide
DSC	differential scanning calorimetry
EIFS	exterior insulation finishing system
FTIR	Fourier transform infrared spectroscopy
MDI	methylene diphenyl diisocyanate
NMR	nuclear magnetic resonance
PEG	polyethylene glycol
PPG	polypropylene glycol
PU	polyurethane
SD	standard deviation
SEM	scanning electron microscopy
T_g	glass transition temperature
TGA	thermogravimetric analysis
TTs	test tubes
XPS	extruded polystyrene

1. Introduction

Within the frame of the global commitment to achieving zero emissions by 2050 (Net Zero Emissions by 2050 Scenario, NZE Scenario, [1]) current building construction practices necessitate an evaluation. As the world strives towards a carbon-neutral future, the choices made in construction materials and design become pivotal in contributing to the overarching aim of reducing carbon footprints [2–5]. Specifically, in modern construction, the fusion of aesthetics and functionality plays a key role in shaping architectural landscapes [6]. In this sense, stone facade cladding is an example of respectful construction practices that align with achieving environmental goals [7], as it has a natural origin. Sandstone, in particular, is a yellowish characteristic stone, easily tailored in slabs or tiles, that captivates the eye and can preserve and enlarge the lifetime of traditional facade isolating materials, like expanded polystyrene panels, reducing the need for frequent replacements and minimise environmental impact [8].

Extruded polystyrene foam (XPS) is known for its lightweight and excellent insulation properties [9]. XPS panels in decorative facades contribute significantly to improving energy efficiency due to their outstanding thermal barrier properties, helping to regulate indoor temperatures and reducing the reliance on artificial heating or cooling systems [7,10–12]. Therefore, these panels enhance the comfort of occupants and diminish energy consumption, also during transportation due to their lightweight (XPS ~30 kg/m^3) compared to other insulating materials like stone wool (70–220 kg/m^3), two high-impact variables in the broader context of sustainable building practices [13]. Moreover, as it was stated before, sandstone-XPS synergy combines aesthetics and enhanced functionality.

To guarantee durability and resilience against environmental elements of the XPS-sandstone panels (Fig. 1a), the attachment

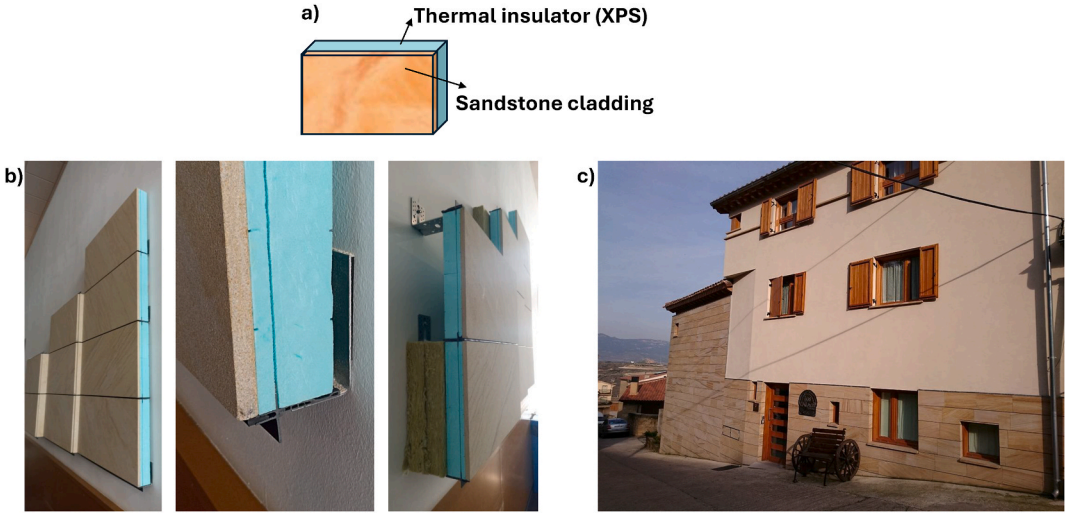

Fig. 1. a) Scheme of insulating panels composed of XPS and sandstone. b) Demonstrator of facade installation made of XPS and sandstone panels (photograph taken at the University of Burgos). c) Example of an insulated building using these types of panels (photograph taken in Vilviestre del Pinar, Spain).

system is paramount. On the one hand, installing facades with panels generally entails utilising the systems depicted in Fig. 1b. Examples of the resulting facades are shown in Fig. 1c. On the other hand, the integrity of these facades relies as well on the sandstone's adhesion to XPS. Presently, polyurethane (PU) adhesives are employed for this specific purpose. They provide strong adhesion and are valued for their durability, flexibility, water resistance, and ability to withstand diverse environmental conditions [14–16].

The manufacturers of XPS-sandstone panels have conveyed the necessity of developing new adhesives that enable the use of satin-finished XPS in the production of these panels. This indicates the absence of such adhesives in the market, thereby underscoring the novelty of our study. Currently, when conventional adhesives are used to bond XPS to stone, the surface of the XPS is sanded to open the pores and create a reticulated surface. This step is crucial to ensure a strong and durable connection between the XPS and the stone, as it facilitates the penetration of the adhesive, thereby allowing it to effectively bond both materials.

After the sanding process, the resulting polystyrene is known in the industry as the Exterior Insulation Finishing System (EIFS). However, for the purposes of this work, we will refer to it as sanded XPS. Production of sanded XPS is a real problem with a prejudicial economic impact in terms of not only rising material manufacturing costs but also increasing material waste. As a matter of fact, sanded XPS is between 30 % and 50 % more expensive per square meter compared to unsanded or satin-finished XPS. At the same time, together with the higher material waste, sanded XPS consumes an expected higher quantity of adhesive, contributing as well to the final product price.

Therefore, it becomes highly important to develop an adhesive that can maintain adhesive strength between sanded XPS and sandstone, but unsanded virgin XPS should be used to avoid increased costs associated with sanding and prevent material waste. This achieves a balance between effective adhesion, economic efficiency, and sustainability for such decorative facades. Hence, the novelty of this work lies in the development of an adhesive demanded by the industry that ensures strong adhesion between satin-finished XPS and stone (Fig. 2). For this purpose, we prepared 6 different catalyst-free adhesives using methylene diphenyl diisocyanate (MDI) and polypropylene glycol (PPG) or polyethylene glycol (PEG) of different molecular weights and characterise their chemical structure and thermal properties. We tested their adhesion properties to bind both satin and sanded XPS to sandstone (extracted from a quarry in Vilviestre del Pinar, Burgos, Spain) and also evaluated the adhesive consumption and the thermal conductivity of the final panel, comparing the results obtained for each type of XPS.

2. Experimental

2.1. Materials

All materials and solvents were commercially available and used as received unless otherwise indicated. The following materials and solvents were used: dimethylsulfoxide-d_6 (99.80 %, VWR), polymeric-MDI (99 %, Voranate M229, DOW, 30 %NCO), polyethylene glycol with average Mn ~2000 (PEG-2000, for synthesis, Merck), polyethylene glycol with average Mn ~1000 (PEG-1000, for synthesis, Merck), polyethylene glycol with average Mn ~600 (PEG-600, for synthesis, Merck), polypropylene glycol with average Mn ~2000 (PPG-2000, Alfa Aesar), polypropylene glycol with average Mn ~1000 (PPG-1000, Alfa Aesar), polypropylene glycol with average Mn ~400 (PPG-400, Thermo Scientific), triethylamine (99 %, VWR).

The used sandstone was a siliciclastic stone (geographical origin in Sierra de Cameros, Vilviestre del Pinar, Burgos, Spain - latitude: 41.951024° N, longitude: 3.078283° W-).

Two types of extruded polystyrene foam (XPS), sanded (6 cm thick) and satin (4 cm thick), were used.

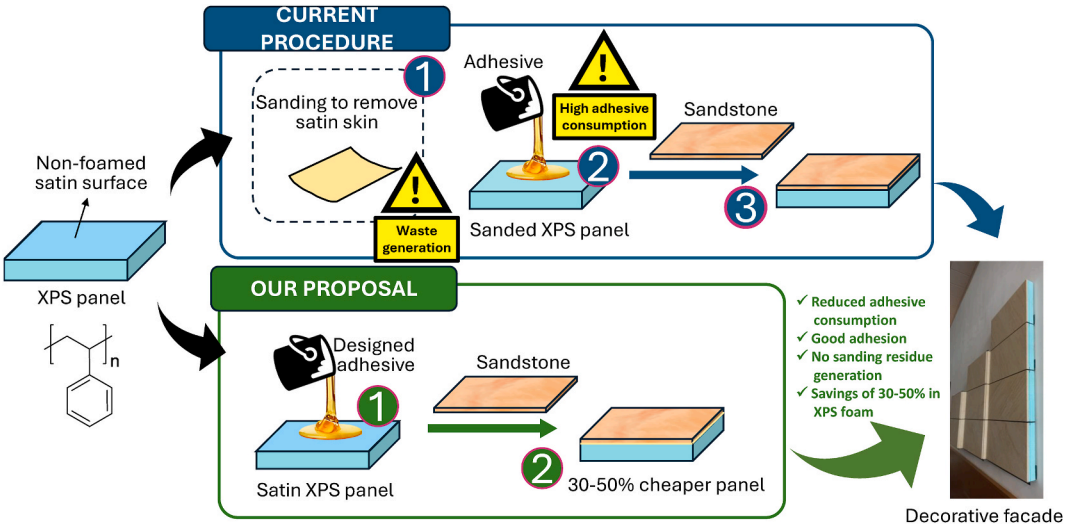

Fig. 2. (top) Illustrative diagram of the current manufacturing process of these sandstone insulation panels with sanded XPS foam, where the satin skin is mechanically removed in the first step, then the adhesive is applied, and finally, XPS and sandstone are bonded. (bottom) A proposed process where sanding of the satin skin is eliminated, and adhesive is applied directly to bond satin-finished XPS and sandstone.

2.2. Instrumentation and general methods

Fig. 3 schematically illustrates the timeline of characterisation techniques used for adhesives, sandstones, foams, and, finally, test tubes simulating facade insulation panels.

The adhesives' isocyanate index (%NCO) was determined in accordance with the ASTM (American Society for Testing and Materials) committee's standard test method titled "Standard Test Method for Isocyanate Groups in Urethane Materials or Prepolymers," specifically the D2572 − 97 (2010) edition.

^{1}H and ^{13}C{^{1}H} nuclear magnetic resonance (NMR) spectra (Advance III HD spectrometer, Bruker Corporation, Billerica, Massachusetts, USA) were recorded at 300 MHz for ^{1}H and 75 MHz for ^{13}C using deuterated dimethylsulfoxide (DMSO-d_6) at 25 °C as solvent.

The thermal characterisation of adhesives, sandstones and foams was conducted using various analytical techniques. Thermogravimetric analysis (TGA) was performed for the adhesives using a Q50 TGA analyser (TA Instruments, New Castle, Delaware, USA). Samples weighing 3–7 mg were subjected to a nitrogen atmosphere with a heating rate of 10 °C·min^{-1}. Differential scanning calorimetry (DSC) was carried out with 15–20 mg samples under a nitrogen atmosphere at a heating rate of 20 °C·min^{-1}, utilising a Q200 DSC analyser (TA Instruments, New Castle, Delaware, USA). The foams' and sandstone's thermal characterisation involved a thermal conductivity analysis in accordance with ASTM C518 and ISO 8301 standards. The analysis was conducted using a FOX50 Heat Flow meter (TA Instruments, New Castle, Delaware, USA). This instrument can accommodate material samples with a maximum thickness of 40 mm and a diameter ranging from 50 to 62 mm. It operates within a temperature range of −10 °C–110 °C, measuring thermal conductivity from 0.1 to 10 W/mK. The measurement is based on quantifying the heat transfer between the two faces of the sample. A good contact between the tested material and the hot plates of the equipment is crucial.

Fourier transform infrared (FTIR) spectra were recorded with an infrared spectrometer (FT/IR-4200, Jasco, Tokyo, Japan) with an attenuated total reflection ATR-PRO410-S single reflection accessory.

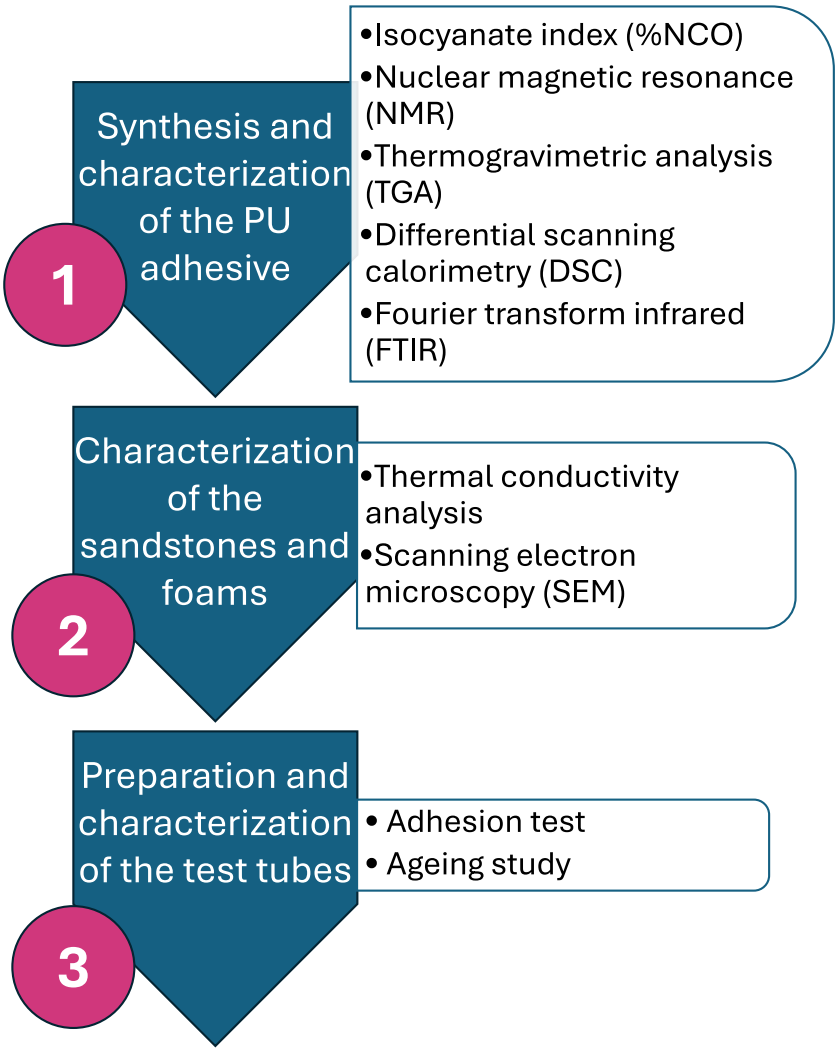

Fig. 3. Flowchart illustrating the different characterisation techniques utilised in the study.

Scanning electron microscopy (SEM) investigations were conducted using an electron microscope (FEI Quanta 600, FELMI-ZFE, Graz, Austria). The foam samples were fractured under liquid nitrogen and gold-sputtered under vacuum to ensure electrical conductivity.

The adhesion test was conducted using an adhesion tester (AT-1000, Neurtek, Eibar, Spain). 4 square sandstone samples of 5 cm side were bonded to a square base of extruded polystyrene (XPS) of 20 cm side (see Fig. 4). In addition, a square steel piece with a 5 cm side and 1 cm thickness was glued to the opposite side of the sandstone. This steel piece was connected to the adhesion equipment, which applied a perpendicular force to the surface until the sandstone and components were separated from the XPS, allowing the determination of strength in MPa.

2.3. Specific methods

2.3.1. Synthesis of adhesives (ADH)

The adhesives (the catalyst-free adhesives) were synthesised in a jacketed glass flask. 86 g of polymeric MDI were added for the fabrication of all adhesives, to which varying amounts of six different polyols were incorporated, as detailed in Table 1. The added quantity of each polyol ensured that the %NCO of the adhesive was 25 %, representing the ratio between isocyanates and hydroxyl groups. After adding the polyol, the mixtures were magnetically stirred for 3 h at 60 °C under a nitrogen atmosphere. Large magnetic stirrers were employed, facilitating effective homogenisation of the mixture at low speeds (between 150 and 300 RPM). The adhesives were stored at 4 °C.

2.3.2. Manufacturing test tubes for adhesion testing

The preparation method for these test tubes, which mimic facade insulation panels, was developed during this study. It was designed to closely resemble the production method of such products at the industrial level. The differences associated with scaling and the material resources available in a small laboratory were addressed by including sanded foam panels in the study, which are commonly prepared industrially.

20 g of adhesive were weighed in a disposable container, and a foam roller was saturated with the adhesive (the original weights of the roller and the container were recorded). Using the roller (Fig. 4a), the adhesive was evenly applied to the surface of various XPS foams, including both satin and sanded variants. All foams were standardised to dimensions of 20x20 cm. The satin and sanded foams exhibited 40 mm and 60 mm thicknesses, respectively. These dimensions were selected due to their prevalence in the construction industry. The surface area of foam coated with the roller was 200 cm^2. Additionally, with the identical roller, adhesive was applied to stone squares (5 cm per side), of which there were also two variants: stone with a thickness of 2 cm and stone with a thickness of 1.5 cm. After the application, the remaining adhesive in the disposable container and the adhesive absorbed by the roller were weighed to determine the adhesive used in the test. Finally, a complete vial of catalysing solution (Figs. 4b and 5 mL of water + 0.330 mL of triethylamine) is sprayed onto the stone and adhesive-coated XPS foam areas, and the parts are bonded (Fig. 4c). As a weight, a glass vial with 100 mL of water on top of each stone is left overnight (Fig. 4d; the total weight of the vial is 261 g). The test tubes (TTs) were tested one week after their preparation. In the SF-VIDEO file, the preparation method for the test tubes can be observed.

2.3.3. Ageing study

To evaluate the behaviour under environmental conditions, we have prepared 3 testing tubes as stated before and submitted them under heat, cold and humidity. 4 sandstone samples were glued to satin XPS, using the adhesive with the higher performance. After the standard sticking process described in the previous section, the test tube was placed in a heater at 80 °C for 3 days. Another testing tube was placed in a freezer at −20 °C for 3 days. In the end, the last test tube was submerged upside down in water for 3 days to test the adhesive water resistance. After this time, the samples were left to temper at ambient conditions for 1 day, and then the resistance to adhesion was measured.

These ageing tests are not included in any official standards as of the publication date of this article, but they are tests that satisfy both producers and customers. In our study, we were advised by industry companies to carry out these procedures.

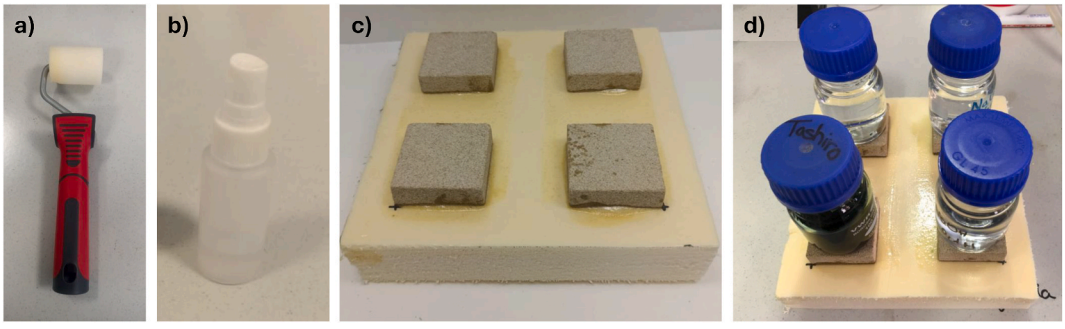

Fig. 4. The figure illustrates various stages and tools employed in the preparation of test tubes for adhesive testing, including: a) the roller used for adhesive application, b) the vial for spraying the catalysing solution, c) the test tube, and d) the test tube with the weights used to achieve proper adhesion.

Table 1
Quantities of polymeric MDI, polyethylene glycol (PEG), and polypropylene glycol (PPG) used in the preparation of different adhesives (ADH).

	ADH_1	ADH_2	ADH_3	ADH_4	ADH_5	ADH_6
Polymeric MDI (g)	86	86	86	86	86	86
PEG, MW: 2000 (g)	14.7	–	–	–	–	–
PPG, MW: 2000 (g)	–	14.7	–	–	–	–
PEG, MW: 1000 (g)	–	–	12.9	–	–	–
PPG, MW: 1000 (g)	–	–	–	12.9	–	–
PEG, MW: 600 (g)	–	–	–	–	11	–
PPG, MW: 400 (g)	–	–	–	–	–	9.4

3. Results and discussion

The synthesised adhesives have a highly similar chemical composition, and as a result, the FTIR and NMR spectra of all of them are very alike (see Fig. 5). In both techniques, the most notable differences are related to the building blocks of the polyols. Adhesives manufactured using polypropylene glycols (i.e. adhesives 2, 4 and 6) exhibit characteristic signals of the pending CH_3 group in FTIR. Signals at around 2970 cm^{-1} can be assigned to ν_{as} CH_3, as well as the signal at 1371 cm^{-1} can be assigned to δ_s CH_3 vibrational mode [17]. In the NMR spectra of adhesives 2, 4 and 6, the signals around 1.08 ppm correspond to lateral methyl groups [18]. Regarding PEG-based adhesives (i.e., adhesives 1, 3 and 5), it is possible to identify a characteristic deformation mode at around 946 cm^{-1} assigned to CH_2–CH_2 bonding, which is highly characteristic of this type of polymer [19]. In Fig. 5a and b, only adhesives 1 and 2 have been represented to show the explained differences, but the same is observable in the remaining adhesives.

Fig. 5c and d depict the adhesive thermal characterisation by TGA and DSC, respectively. As shown by TGA, the greater the polyol molecular weight, the lower the thermal stability of the adhesive. This behaviour can be explained in terms of chain cleavage, as the longer the chain, the more probable the thermal breaking points affecting the stability of the polymer. When comparing the nature of the polyols, the pending methyl group in PPG-based adhesives affects the stacking capability of the polymeric chains. Consequently, PEG-based adhesives have higher thermal stability than PPG counterfeits. The DSC tests reveal similar behaviours for all adhesives, with an apparent glass transition temperature (T_g) at approximately −30 °C. This glass transition temperature is intrinsic to poly-MDI, and, logically, all adhesives exhibit it, as it is the major component.

In Fig. 5e, SEM images for both sanded and satin foam can be seen. The cross-sectional analysis reveals, as expected, a structure of closed pores in both cases, which is very common in thermal insulation materials. However, there is a considerable difference when comparing the surface of the foams. While the satin foam has a smooth surface, the sanded foam presents the surface's structural pores, as the smooth satin skin has been mechanically removed.

Consequently, all of them are comparable, and two types of conclusions are elaborated upon in the following sections of this paper. The first one aims to determine how the molecular weight of the polyols (ranging from 400 to 2000) affects the obtained adhesion. The second one investigates how the chemical nature of the polyol (PEG or PPG) impacts adhesion.

3.1. Adhesion results

Table 2 summarises the results obtained in the adhesion tests. The control parameters were the nature of the polyols (PEG or PPG) and their molecular weight (ranging from 400 to 2000), which resulted in six different adhesives, the sandstone thickness (2 or 1.5 cm), and the type of XPS (satin or sanded). Additionally, it depicts the amount of adhesive used in the preparation of each test tube, as well as the type of stone, foam, and adhesive employed.

The first noteworthy finding that can be gleaned from these results pertains to the amount of adhesive used, which is visually depicted in Fig. 6a. When sanded foam is employed, the adhesive expended in a test tube is more than 2 times greater than the adhesive consumption observed with satin foam (8.55 ± 2.17 and 3.86 ± 1.96 g, respectively). When these quantities are extrapolated to g m^{-2}, the use of sanded foam would result in a consumption rate of approximately 684 g m^{-2}, while with satin foam, it would be a mere 309 g m^{-2}. This result was expected after the SEM image characterisation, as the sanded foam has a completely porous surface, and the adhesive can penetrate the lattice, which leads to a significant increase in adhesive consumption.

The difference in adhesive consumption is not reflected in the adhesive strength between the different foams and the stone. In fact, the average tensile strength in the test when using sanded foam is 0.45 ± 0.09 N mm^{-2} (similar to that reported by industry companies), and it reaches a value of 0.39 ± 0.08 N mm^{-2} when using satin foam. In other words, these values are very similar, as shown in Fig. 6b. Moreover, each test tube is replicated four times, resulting in 96 adhesion tests conducted, out of which only 18 tests experienced adhesive failure. Stated differently, 81 % of the test probes failed due to the limiting intrinsic tensile strength of stone or foam material, as depicted in Fig. 6c, demonstrating the adhesive's significant adhesive bonding capability.

Another expected result was the lack of a difference in the adhesion test between the test tubes made with 2 cm thick stone (thick stone) and those made with 1.5 cm thick stone (thin stone). When comparing the results from all 24 test tubes, an average adhesion value of 0.41 ± 0.09 N mm^{-2} was obtained with thick stone, while thin stone yielded an average adhesion value of 0.42 ± 0.09 N mm^{-2}.

From a chemical perspective, specifically from a materials science standpoint, it is highly intriguing to examine the difference in adhesion between adhesives manufactured with PEG compared to adhesives manufactured with PPG (Fig. 6d). While all the results are favourable since all adhesives could be utilised for the manufacturing of sandstone-XPS panels, it is indeed evident from the results that there is a tendency towards higher tensile strength when using PPG. The two best-performing adhesives in terms of tensile strength in

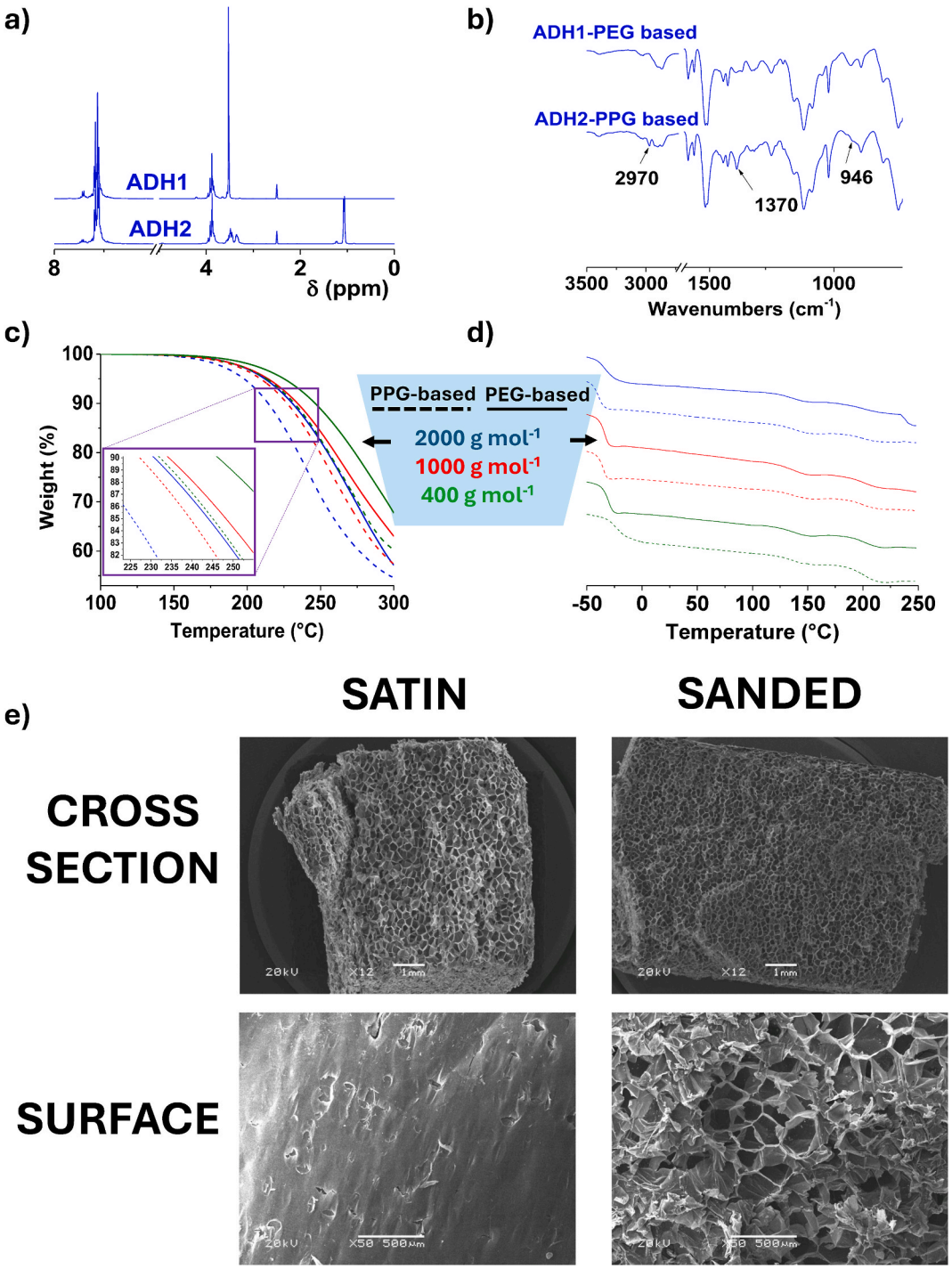

Fig. 5. **a)** H^1-NMR differences between PEG and PPG-based adhesives; **b)** FTIR characteristic signals of PEG and PPG-based adhesives; **c)** adhesives' thermogravimetric curves at 10 °C min^{-1} under nitrogen atmosphere; **d)** adhesives' DSC curves at a heating rate of 20 °C min^{-1} under a nitrogen atmosphere; **e)** SEM images of satin and sanded foams (cross-section and surface).

the adhesion test are those manufactured with PPG-1000 and PPG-2000. This is associated with the rigidity imposed by the lateral methyl group of PPG, which results in steric hindrance that translates into rotation impediments and, therefore, rigidity.

Considering the molecular weights, it appears that the behaviour in terms of adhesion is the same for adhesives based on PPG as for those based on PEG. Fig. 6d shows a maximum tensile strength when using molecular weights of 1000. Our interpretation is that the adhesive must meet two basic requirements. Firstly, it should penetrate the micropores of both surfaces relatively easily, which is

Table 2
Description of the materials used in the preparation of each test tube (TT) concerning the adhesive used (ADH), type of sandstone (coarse or fine), type of XPS (satin or sanded), and amount of adhesive applied between foam and sandstone. The table shows the results of the adhesion resistance tests for each specimen. Data are means of four replicates ± SD.

Test Tubes	Adhesive	Sandstone thickness		XPS type		Amount of adhesive consumed (g)	Resistance in the adhesion test (N/mm^2)		
		2 cm	1.5 cm	Sanded	Satin				
TT_1	ADH_2	✓		✓		8.54	0.35	±	0.02
TT_2	ADH_2	✓			✓	8.81	0.46	±	0.05
TT_3	ADH_2		✓	✓		2.76	0.55	±	0.14
TT_4	ADH_2		✓		X	2.69	0.44	±	0.08
TT_5	ADH_1		✓		✓	2.68	0.29	±	0.10
TT_6	ADH_1		✓	✓		8.59	0.48	±	0.06
TT_7	ADH_1	✓			✓	2.98	0.40	±	0.03
TT_8	ADH_1	✓		✓		8.34	0.40	±	0.07
TT_9	ADH_3	✓		✓		9.44	0.49	±	0.09
TT_10	ADH_3		✓		✓	6.75	0.34	±	0.06
TT_11	ADH_3	✓			✓	4,32	0.45	±	0.04
TT_12	ADH_3		✓	✓		11.57	0.42	±	0.05
TT_13	ADH_4	✓		✓		10.83	0.61	±	0.11
TT_14	ADH_4		✓		✓	2.55	0.44	±	0.09
TT_15	ADH_4	✓			✓	2.56	0.52	±	0.04
TT_16	ADH_4		✓	✓		9.1	0.51	±	0.08
TT_17	ADH_5	✓		✓		8.15	0.35	±	0.07
TT_18	ADH_5	✓			✓	3.58	0.30	±	0.08
TT_19	ADH_5		✓	✓		9.7	0.34	±	0.02
TT_20	ADH_5		✓		✓	2.92	0.28	±	0.04
TT_21	ADH_6	✓		✓		7.77	0.43	±	0.06
TT_22	ADH_6	✓			✓	3.81	0.36	±	0.04
TT_23	ADH_6		✓	✓		7.8	0.49	±	0.08
TT_24	ADH_6		✓		✓	2.66	0.42	±	0.13

favoured in flexible adhesives. On the other hand, adhesive strength is higher when adhesives are rigid. Therefore, balancing flexible segments (polyols) and rigid segments (poly-MDI) is essential. In the case of low molecular weight polyols, the rigid portion is overly represented in the adhesive, hindering proper penetration into the surface micropores. In the case of adhesives with high molecular weight polyols, penetration is good, but they are too flexible. With polyols of molecular weights centred around 1,000, the ideal balance between rigid and flexible sequences is achieved, providing good penetration on both surfaces while maintaining the necessary rigidity to achieve good adhesive properties. Nevertheless, the most significant conclusion from this section of the article, and likely from the entire study, is that these adhesive types effectively address the issue highlighted in the introduction. They enable the utilisation of satin XPS in manufacturing such panels, which can yield economic benefits, as sanded XPS is 30–50 % more expensive.

3.2. Adhesion test after accelerated ageing

The adhesion resistance of the aged testing tubes was evaluated. According to the results, the best performing adhesive was PPG 1000 polyurethane. 4 thick sandstone samples were glued to satin XPS with ADH4. The adhesive consumption for each of the ageing testing tubes was, as expected, 2.75 g for the heated sample, 2.98 g for the cooling sample and 2.90 g for the underwater ageing sample. The adhesive consumption was in agreement with our previous observations.

With regard to the adhesion resistance, in Fig. 7a, the resistance to adhesion after ageing has been depicted. At first sight, it seems that the previous high performance has been prejudiced in around 30 % of the cohesive force. However, the influence of environmental factors on XPS and stone separately was not taken into account. In Fig. 7b, c and 7d, it can be seen that all of the failures were not adhesive failures, i.e., the resistance to adhesion is the breaking point at which the stone or the foam breaks. In this sense, the adhesion strength is higher than the resistance of XPS or sandstone tensile strength. This very promising result reveals that in harsh environmental conditions, the adhesive does not suffer as much as the materials do separately.

3.3. Thermal conductivity results

The thermal conductivity of each material was measured separately, following the standard UNE-EN 12667: Thermal performance of building materials and products. Determination of thermal resistance by means of guarded hot plate and heat flow meter methods. Products of high and medium thermal resistance.

The XPS foam is expected to present a much higher insulating capacity than the sandstone. Therefore, the foam would direct the glued decorative panels' properties. Four different sandstone blocks of 15 mm thick were measured, each replicated 10 times. Sandstone presents a mean thermal conductivity value of 1.43 W/mK, so it has an intermediate conductivity value, as it is between 0.1 and 2 W/mK, which are the values set by the standards. The XPS sanded and satin foams have similar mean values, 0.03 and 0.05 W/mK, respectively, making it a very insulating material since it is below the standard's 0.1 W/mK limit. The slight difference in thermal

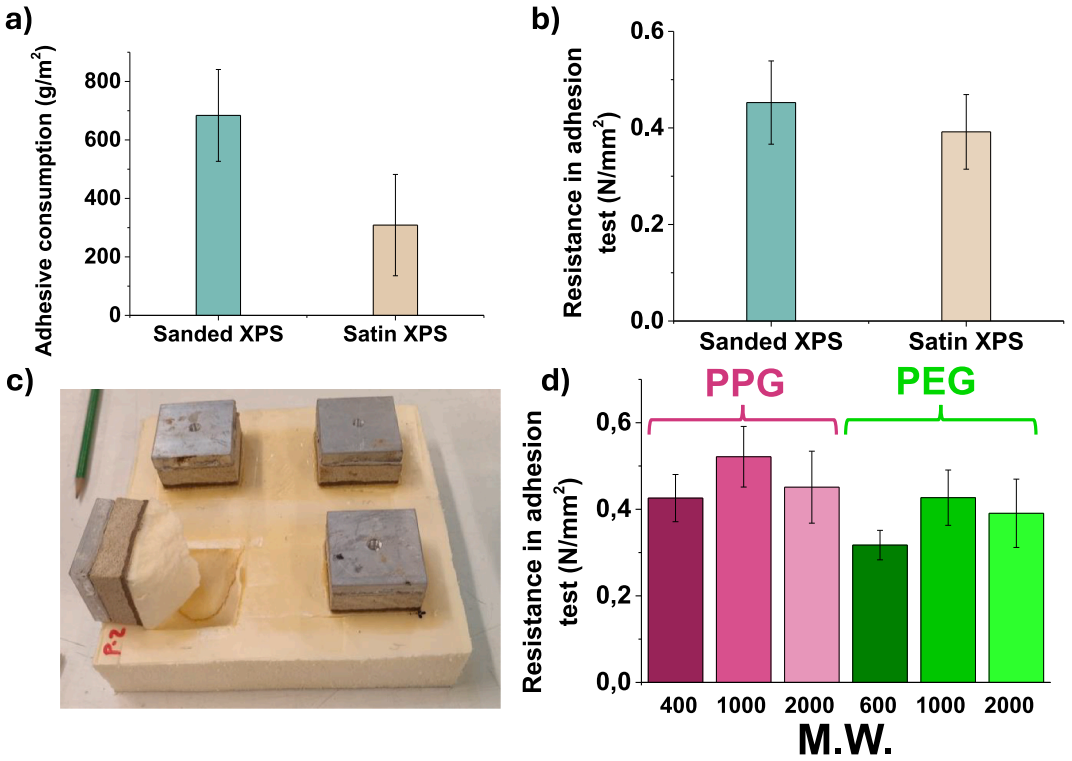

Fig. 6. **a)** Adhesive consumption when preparing the test tubes with satin foam and sanded foam; **b)** tensile strength in the adhesion tests for the test tubes with satin foam and sanded foam; **c)** Image of one of the test tubes after conducting one of its four adhesion tests, showing the fracture of the satin XPS foam; **d)** representation of tensile strength in adhesion tests as a function of the different polyols used in adhesive manufacturing. All data are means of four replicates ± SD.

conductivity between the foam samples is not significant, and we suspect it is due to the contact between the hot plates of the measuring equipment and the foam. In the case of the satin foam, the contact is perfect, whereas in the case of the sanded foam, it is not as effective.

4. Conclusions

In this study, we evaluated different polyurethane-based adhesives to enhance the adhesion properties between decorative sandstone and XPS insulation panels. Thanks to the improved adhesion properties of these adhesives, it is possible to obtain decorative insulation panels for facades from satin-finished XPS foams. This method offers cost-saving advantages compared to panels made from sanded foams priced 30–50 % higher than satin XPS. The variables evaluated in this work include the molecular weight and the nature of the aliphatic chain of the polyols used. Regarding molecular weight, the tensile strength results reveal that PEG and PPGs of 1000 g mol^{-1} allow the most convenient equilibrium between the rigidity of MDI aromatic rings and the flexibility of aliphatic glycol chains. When comparing the aliphatic nature of the polyols, polyurethanes derived from polypropylene glycols resulted in improved tensile strength compared to those derived from polyethylene glycol. In addition to being a more economical material, the adhesive consumption is lower in satin-finished foam panels than in sanded foam panels. Moreover, the maintained high-performance behaviour of the best adhesive after harsh environmental conditions, namely under continuous high temperature, cold and underwater, opens the possibility of further studying the adhesive's behaviour under outdoor exposure. Therefore, the adhesives described in this study could be used in insulating outdoor decorative panels, both enabling a cost reduction in the XPS material and significantly impacting more sustainable constructions by reducing adhesive consumption.

Open Data

Open Data is available at https://riubu.ubu.es/handle/10259/5684 under the name "UBU-Polymers Research Group 19022024".

CRediT authorship contribution statement

Álvaro Miguel-Ortega: Writing – original draft, Validation, Investigation. **Sara Gonzalez-Moreno:** Writing – original draft, Validation, Methodology. **Jose Manuel Gonzalez-Martin:** Supervision, Methodology, Funding acquisition, Conceptualization. **Raquel Arroyo:** Writing – original draft, Resources, Methodology. **Félix C. García:** Writing – review & editing, Supervision, Conceptualization. **Miriam Trigo-Lopez:** Writing – original draft, Validation, Methodology, Investigation, Formal analysis. **Saúl Vallejos:** Writing – review & editing, Writing – original draft, Supervision, Project administration, Methodology, Investigation,

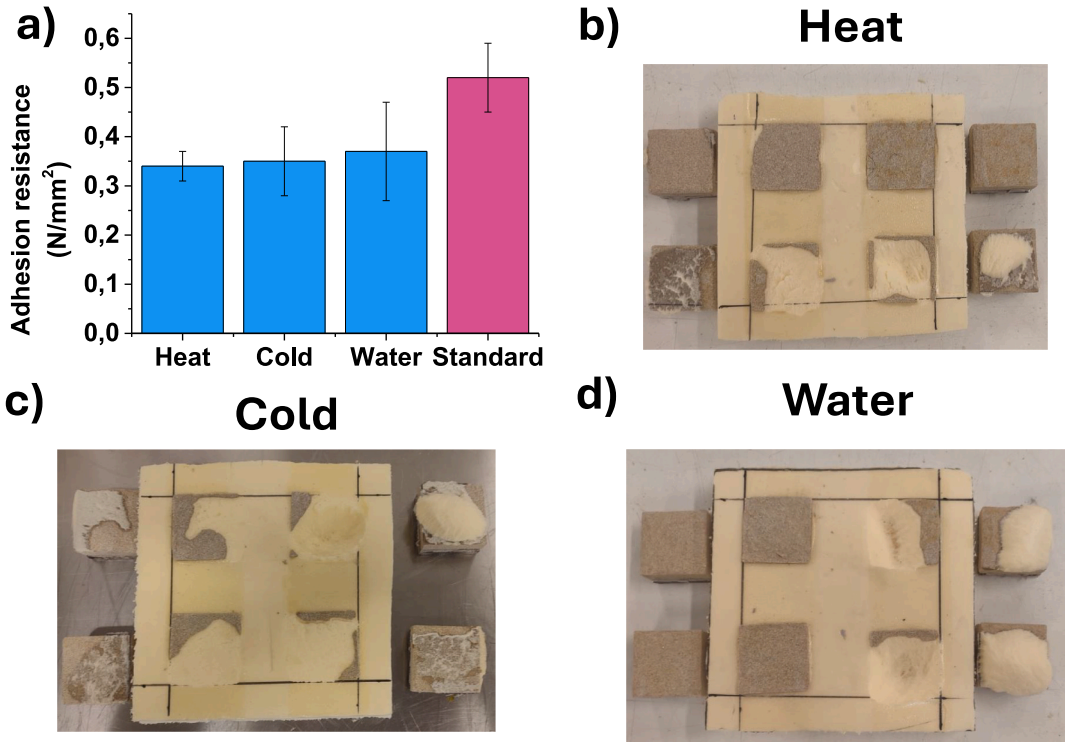

Fig. 7. a) Resistance adhesion result after environmental accelerated ageing of ADH4 with sandstone glued to satin XPS; b) adhesion results after subjecting the sample to a temperature of 80 °C for 3 days; c) adhesion results after subjecting the sample to a temperature of −20 °C for 3 days; and d) adhesion results after fully immersing the sample in water for 3 days.

Funding acquisition, Conceptualization.

Declaration of competing interest

The authors declare that they have no known competing financial interests or personal relationships that could have appeared to influence the work reported in this paper.

Data availability

No data was used for the research described in the article.

Acknowledgements

We gratefully acknowledge the financial support provided by all funders. This work was supported by the Regional Government of Castilla y León (Junta de Castilla y León) and by the Ministry of Science and Innovation MICIN and the European Union NextGenerationEU PRTR. Author Saul Vallejos received grant BG22/00086 funded by the Spanish Ministerio de Universidades. Author Álvaro Miguel's work was facilitated by the Margarita Salas grant (CA1/RSUE/2021–00409), funded by the Universidad Autónoma de Madrid. The financial support provided by Fondo Europeo de Desarrollo Regional-European Regional Development Fund (FEDER, ERDF) and Regional Government of Castilla y León -Consejería de Educación, Junta de Castilla y León- (BU025P23) is gratefully acknowledged. We also acknowledge the funding provided by Grant PID2020-113264RB-I00 funded by MCIN/AEI/10.13039/501100011033 and by "ERDF A way of making Europe".

Appendix A. Supplementary data

Supplementary data to this article can be found online at https://doi.org/10.1016/j.jobe.2024.110301.

References

[1] International Energy Agency, Net zero by 2050: a roadmap for the global energy sector, Int. Energy Agency (2021) 70. https://iea.blob.core.windows.net/assets/deebef5d-0c34-4539-9d0c-10b13d840027/NetZeroby2050-ARoadmapfortheGlobalEnergySector_CORR.pdf.

[2] A. Kumar, B.M. Suman, Experimental evaluation of insulation materials for walls and roofs and their impact on indoor thermal comfort under composite climate, Build. Environ. 59 (2013) 635–643, https://doi.org/10.1016/J.BUILDENV.2012.09.023.
[3] A. Briga-Sá, D. Nascimento, N. Teixeira, J. Pinto, F. Caldeira, H. Varum, A. Paiva, Textile waste as an alternative thermal insulation building material solution, Construct. Build. Mater. 38 (2013) 155–160, https://doi.org/10.1016/J.CONBUILDMAT.2012.08.037.
[4] B. Sizirici, Y. Fseha, C.S. Cho, I. Yildiz, Y.J. Byon, A review of carbon footprint reduction in construction industry, from design to operation, Materials 14 (2021) 6094, https://doi.org/10.3390/MA14206094.
[5] R. Hasanzadeh, T. Azdast, P.C. Lee, C.B. Park, A review of the state-of-the-art on thermal insulation performance of polymeric foams, Therm. Sci. Eng. Prog. 41 (2023) 101808, https://doi.org/10.1016/J.TSEP.2023.101808.
[6] Y. Li, S. Ren, Building Decorative Materials, Elsevier Ltd, 2011, https://doi.org/10.1533/9780857092588.
[7] E. Franzoni, B. Pigino, G. Graziani, C. Lucchese, A. Fregni, A new prefabricated external thermal insulation composite board with ceramic finishing for buildings retrofitting, Mater. Struct. 49 (2016) 1527–1542, https://doi.org/10.1617/S11527-015-0593-7/TABLES/9.
[8] D. Fernando, S. Navaratnam, P. Rajeev, J. Sanjayan, Study of technological advancement and challenges of façade system for sustainable building: current design practice, Sustainability 15 (2023) 14319, https://doi.org/10.3390/SU151914319.
[9] A.D.R. Pontinha, J. Mäntyneva, P. Santos, L. Durães, Thermomechanical performance assessment of sustainable buildings' insulating materials under accelerated ageing conditions, Gels 9 (2023) 241, https://doi.org/10.3390/GELS9030241.
[10] S. Schiavoni, F. D'Alessandro, F. Bianchi, F. Asdrubali, Insulation materials for the building sector: a review and comparative analysis, Renew. Sustain. Energy Rev. 62 (2016) 988–1011, https://doi.org/10.1016/J.RSER.2016.05.045.
[11] B.P. Jelle, Traditional, state-of-the-art and future thermal building insulation materials and solutions – properties, requirements and possibilities, Energy Build. 43 (2011) 2549–2563, https://doi.org/10.1016/J.ENBUILD.2011.05.015.
[12] Y. Dong, J. Kong, S. Mousavi, B. Rismanchi, P.S. Yap, Wall insulation materials in different climate zones: a review on challenges and opportunities of available alternatives, Thermoelectrics 3 (2023) 38–65, https://doi.org/10.3390/THERMO3010003.
[13] M. Rawat, D. Singh, S. Singh, D. Buddhi, Thermal insulation materials and its energy savings aspects for building envelopes: a review, AIP Conf. Proc. 2771 (2023) 20039, https://doi.org/10.1063/5.0152267/2908805.
[14] H.M.C.C. Somarathna, S.N. Raman, D. Mohotti, A.A. Mutalib, K.H. Badri, The use of polyurethane for structural and infrastructural engineering applications: a state-of-the-art review, Construct. Build. Mater. 190 (2018) 995–1014, https://doi.org/10.1016/J.CONBUILDMAT.2018.09.166.
[15] C. Strobech, Polyurethane adhesives, Construct. Build. Mater. 4 (1990) 214–217, https://doi.org/10.1016/0950-0618(90)90042-Y.
[16] F. Choffat, A. Corsaro, C. Di Fratta, S. Kelch, Advances in polyurethane structural adhesives, in: Adv. Struct. Adhes. Bond, second ed., Woodhead Publishing, 2023, pp. 103–136, https://doi.org/10.1016/B978-0-323-91214-3.00032-6.
[17] J. Fang, L. Zhang, D. Sutton, X. Wang, T. Lin, Needleless melt-electrospinning of polypropylene nanofibres, J. Nanomater. 2012 (2012) 382639, https://doi.org/10.1155/2012/382639.
[18] A. Prabhakar, D.K. Chattopadhyay, B. Jagadeesh, K.V.S.N. Raju, Structural investigations of polypropylene glycol (PPG) and isophorone diisocyanate (IPDI)-based polyurethane prepolymer by 1D and 2D NMR spectroscopy, J. Polym. Sci. Part A Polym. Chem. 43 (2005) 1196–1209, https://doi.org/10.1002/POLA.20583.
[19] E. Finocchio, C. Cristiani, G. Dotelli, P.G. Stampino, L. Zampori, Thermal evolution of PEG-based and BRIJ-based hybrid organo-inorganic materials. FT-IR studies, Vib. Spectrosc. 71 (2014) 47–56, https://doi.org/10.1016/J.VIBSPEC.2013.12.010.